

Few-Shot Unlearning by Model Inversion

Youngsik Yoon^{1*}, Jinhwan Nam^{2*}, Hyojeong Yun¹, Dongwoo Kim^{1,2}, Jungseul Ok^{1,2}

¹ Department of Computer Science & Engineering, Pohang University of Science and Technology

² Graduate School of Artificial Intelligence, Pohang University of Science and Technology

Abstract

We consider the problem of machine unlearning to erase a target dataset, which causes an unwanted behavior, from the trained model when the training dataset is not given. Previous works have assumed that the target dataset indicates all the training data imposing the unwanted behavior. However, it is often infeasible to obtain such a complete indication. We hence address a practical scenario of unlearning provided a few samples of target data, so-called *few-shot unlearning*. To this end, we devise a straightforward framework, including a new model inversion technique to retrieve the training data from the model, followed by filtering out samples similar to the target samples and then relearning. We demonstrate that our method using only a subset of target data can outperform the state-of-the-art methods with a full indication of target data.

1 Introduction

Machine unlearning is a task to excise a target dataset from a machine learning model when the target data, such as mislabeled or malicious samples (e.g., [3, 7]) or a specific type of data of privacy concerns (c.f., right to be forgotten [21]), is suspected of inducing an unwanted behavior in the process of training. A straightforward approach is retraining the model from scratch with the data remaining after excluding the target. However, this is often restricted mainly due to limited access to (i) the entire data; or (ii) the target data. For instance, in a continual learning framework with a stream of data, memory cost and privacy concerns make it difficult to store the entire training data or to indicate all the malicious data to be erased. Hence, a standard unlearning problem [12, 23, 9] is posed and addressed only with the trained model and target data, i.e., the training data is not given.

Despite such extensive efforts, it is still challenging in practice to *target* and unlearn only the unwanted behavior from the model using the existing methods [12, 9]. This is mainly because the *target behavior* is specified by not only target data but also critical hyperparameter (say λ) quantifying the overall influence of target data under their problem formulations, whereas a careful search of λ is limited due to the absence of training data to estimate the validity of λ . To bypass such a vagueness about what to unlearn from the model, we explicitly postulate a target behavior which can be exemplified by a few samples, and formulate a *few-shot unlearning* problem. This is indeed a practical scenario as it is impractical to track down all the data which have induced the target behavior into the model.

Contributions. For the few-shot unlearning problem (Section 2), we propose a straightforward framework (Section 3) consisting of (i) *model inversion* to retrieve a proxy for training data from the given model; (ii) *filtration* to exclude a part of the retrieved data potentially inducing the unwanted behavior while interpolating the few target samples; and then (iii) *relearning* with the filtered data. Specifically, as the model inversion problem is often under-determined, we devise a new technique (Section 3.1) which trains a generator of the latent data distribution using an extensive set of side-information possibly extracted from the trained model. This can be of independent interest in various learning problems such as data-free transfer learning [30]. We note that such an intuitive design

* equal contribution

with model inversion enables us to easily debug the unlearning result step-by-step. Our experiments (Section 4) demonstrate the superiority of our method on various settings compared to existing ones dedicated to either Bayesian learning models [23] or typical deep learning models [12]. While the existing ones often fail at erasing the unwanted behavior or distort the accuracy on remaining data, ours shows unlearning result constantly close to the oracle which has full access to training and target data.

1.1 Related Work

Existing formulations of machine unlearning. Various levels of accessibility to training data D and target data D_e have been considered and formulated different unlearning problems [2, 15, 14, 16, 11, 27, 10, 12, 23, 9, 1, 6]. In [2, 14, 16, 27], assuming full access to D and D_e (i.e., no difficulty to obtain and remember D_r), the unlearning problem mainly is focused on how to reduce the computational cost of unlearning compared to relearning D_r from scratch. For the case with no access to D [12, 23, 9, 1, 6], the crux is to prevent catastrophic forgetting on remaining data $D_r := D \setminus D_e$, while successfully erasing the influence of D_e on the original model. However, without retrieving D , it is inevitable to have a hyperparameter λ governing the overall magnitude of influence of D_e for the model is trained upon not only canonical deep learning [12] but also Bayesian deep learning with a relatively rich clue on D [23]. In other words, only when the influence of D_e under a subtle choice of λ tightly corresponds to the target behavior being unwanted, we can avoid either skimpy or overkill unlearning. We hence stipulate the target behavior first and then formulate the few-shot unlearning problem to remove the target behavior from its few examples. Similar to our formulation, zero-shot unlearning [6] has no ambiguity on the target behavior described by class(es) to be forgotten even without any sample data. However, it is applicable only when we want the model to fail at classifying some classes, i.e., it cannot unlearn a sophisticated target behavior that ours can address.

Other applications of model inversion. With scaling machine learning data and increasing attention on privacy concerns, model inversion has been widely studied in various contexts of machine learning [30, 4, 29, 5, 20, 31, 32, 8, 28, 18]. The model inversion is particularly useful in *data-free* transfer learning, required for model compression [30, 4, 29, 5, 20, 31, 32] and continual learning [29], where we want to distill the knowledge of the trained model into another but have no training data. In addition, to check privacy leakage, one can formulate the problem of inverting data from model [8, 28] or even gradient [18], where a number of prior information about the data domain have been considered to reduce the searching space of inversion problem. Our inversion method is the first to train a remarkable generator to approximate the training data distribution of a given model with the most complete set of side-information (batch norm statistics, data augmentation, and total variance) available in a common deep learning model. To our best knowledge, our work is the first to propose model inversion and filtration using the semantic consistency prior of data augmentation. Hence, as aforementioned, this is of independent interest for not only unlearning but also other data-free scenarios.

2 Problem Formulation

Standard unlearning. We consider a standard classification data $D = \{d_i = (x_i, y_i)\}_{i=1}^N$, where $x_i \in \mathcal{X}$ is input data such as an image and $y_i \in \mathcal{Y} := \{1, 2, \dots, K\}$ is its corresponding label. Let $f_{w_o}(\cdot) \in [0, 1]^K$ be a classifier of parameter w_o trained on D with the cross-entropy (CE) loss, where we augment the dataset with a set of input data transformations $\{\phi_\ell\}_{\ell=1}^L$ preserving the semantic, e.g., rotation and crop for images, as a canonical technique to enhance generalization ability, i.e.,

$$w_o \in \arg \min_w \sum_{(x_i, y_i) \in D} \sum_k \text{CE}(f_w(\phi_k(x_i)), y_i) . \quad (1)$$

Given w_o and $D_e \subset D$ (without D), the standard unlearning task [23, 12] aims at approximating w_u trained with the same objective in equation 1 but $D_r := D \setminus D_e$ instead of D , i.e.,

$$w_u \in \arg \min_w \sum_{(x_i, y_i) \in D_r} \sum_k \text{CE}(f_w(\phi_k(x_i)), y_i) . \quad (2)$$

This is typically formulated to unlearn an unwanted behavior of w_o imposed by D_e . For instance, letting D_e be the set of all the mislabeled data in training, the goal of unlearning is to correct the

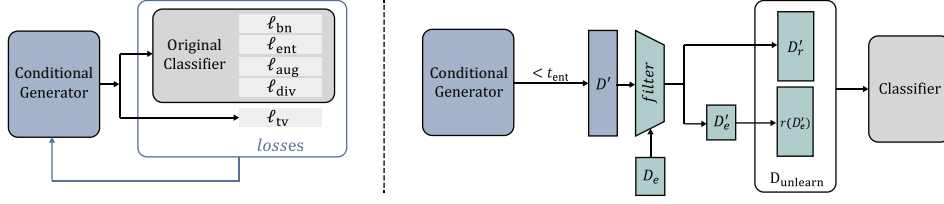


Figure 1: **A concept diagram of proposed method.** The generator is trained by original classifier and overall losses to generate D_e , the approximation of D . The filter from D_e classifies D_e -like samples in generated samples D' , then we modify D' to make D_{unlearn} for unlearning. The classifier unlearns specific data D_e by relearning from D_{unlearn} .

misclassification of w_o influenced by D_e . However, obtaining D_r from w_o and D_e is often under-determined and thus it is inevitable to introduce a sensitive hyperparameter (λ 's in [23, 12]) which determines the relative influence of D_e compared to D_r . To bypass such an ambiguity, we focus on target behavior rather than target data, and formulate *few-shot unlearning* formally described in what follows. Meanwhile, as it is hard to track down every mislabeling or data to be erased in practice, the few-shot unlearning is a practical variant with an incomplete collection of target data.

Few-shot unlearning. Given a target behavior of w_o to be erased, we let D_e be the complete subset of training data exemplifying it, e.g., all the mislabeled data. Let $D_{e,\rho}$ be a subset of D_e such that $\mathbb{E}[|D_{e,\rho}|] \approx \rho|D_e|$. Then, the few-shot unlearning problem given $D_{e,\rho}$ and w_o (without knowing ρ) is naturally defined to be the one seeking for w_u in equation 2 of the standard unlearning with D_e and w_o . It is particularly useful to study the case with small ρ . In such cases, we have $D_{r,\rho} := D \setminus D_{e,\rho} \approx D$, and thus the standard unlearning with $D_{e,\rho}$ is prone to unlearn nothing from the previous model w_o by definition as empirically shown in Figure 2. We finally remark that the few-shot unlearning task needs to address the challenges of the standard unlearning task in addition to those to interpolate the dataset to be erased from the few-shot $D_{e,\rho}$.

3 Proposed Method

In this section, we describe the proposed framework of few-shot unlearning method, illustrated in Figure 1, consisting of two major steps followed by relearning: (i) model inversion; and (ii) filtration. The first step (Section 3.1) is to generate an approximation D' of D to maintain the performance of the model. We introduce the method to train the generator without accessing any training data. The second one (Section 3.2) is to filter out D_e -like samples from the approximation D' . Then, finally, we unlearn D_e from the baseline model by retraining with the filtered approximated dataset. Pseudo code of overall method is provided in Appendix A.

3.1 Data Generation with Model Inversion

We describe how to train a generator to approximate the inaccessible original dataset D in this section. Let $G : \mathcal{Z} \times \mathcal{Y} \mapsto \mathcal{X}$ be a conditional generator which takes a target label $y \in \mathcal{Y}$ and random noise $z \in \mathcal{Z}$ from an arbitrary distribution for sampling output image $x \in \mathcal{X}$. Note that training the conditional GAN [22] is infeasible since we only have access to D_e and thus cannot train a discriminator. Instead, we utilize the information from the trained classifier f_{w_o} to train the conditional generator. To train the generator, we use five different losses capturing our belief on likely input data: entropy loss ℓ_{ent} , augmentation loss ℓ_{aug} , diversity loss ℓ_{div} , batch normalization loss ℓ_{bn} , and total variance loss ℓ_{tv} . We apply these losses to a mini-batch of samples to make the training stable. In what follows, we describe the details of each loss used in training.

Entropy loss. We employ an entropy loss to generate an image that can potentially be classified as the target label used as an input of the conditional generator. Let $B = \{(z_i, y_i)\}_{i=1}^M$ be the mini-batch of randomly sampled noise z and label y . Our entropy loss ℓ_{ent} for mini-batch B is defined as:

$$\ell_{\text{ent}}(B) = \sum_{(z,y) \in B} \text{CE}(f_{w_o}(G(z, y)), y), \quad (3)$$

which encourages G to generate samples that can be predicted as the label y .

Augmentation loss. We assume that the trained classifier f_{w_o} is robust under the data augmentations such as flipping, rotating, and cropping, used in a training step. If the generated samples are similar

to the trained images, then the classification result of f_w on the original and augmented samples need to be similar to each other. Otherwise, the generated samples are unlikely used in training f_{w_o} . To encourage G to generate realistic samples under data augmentation, we define a data augmentation loss ℓ_{aug} for mini-batch B is defined as:

$$\ell_{\text{aug}}(B) = \sum_{(z,y) \in B} \sum_{\phi_k \in \Phi} \|f_{w_o}(G(z,y)) - f_{w_o}(\phi_k(G(z,y)))\|_2^2, \quad (4)$$

where $\Phi = \{\phi_k\}_{k=1}^K$ is a set of K predefined augmentation operations.

Diversity loss. Generator often suffers from the mode-collapsing [13]. In our case, having a few collapsed samples per label can potentially make the unlearning unstable since the coverage of the generated samples is limited. To overcome the issue of mode-collapse, we borrow the diversity loss ℓ_{div} from [30], formally defined as:

$$\ell_{\text{div}}(B) = \sum_{y \in Y} \exp \left(- \sum_{(z_1,y) \in B} \sum_{(z_2,y) \in B} \|z_1 - z_2\|_2^2 \cdot \|f_e(G(z_1,y)) - f_e(G(z_2,y))\|_1 \right), \quad (5)$$

where z_1 and z_2 are two randomly sampled noises, and f_e is a pre-trained network extracting useful behaviors from the given input. In [30], the distance between $G(z_i, y)$ is used instead of $f_e(G(z_i, y))$ in ours. We use f_e for calculating distance, as using the distance between images pixel by pixel can encourage the generator to generate unrealistic images. The diversity loss penalizes G generating similar samples from different noises and thus alleviates the mode-collapse.

Batch normalization loss. Batch normalization(BN) keeps useful statistics of an input dataset at each layer of the neural network. The use of the BN is a de-facto standard in training a classifier, and we also assume the same for f_{w_o} . As proposed in [29], model inversion can utilize BN statistics, which represent a meta-data of D in terms of the running mean and variance. Specifically, the following BN loss ℓ_{bn} forces generated images to fit stored mean and variance, statistics of generated images match to those of real dataset D :

$$\ell_{\text{bn}}(B) = \sum_l \|\mu_l - \mu_{\text{exact}}\|_2^2 + \|\sigma_l^2 - \sigma_{\text{exact}}^2\|_2^2, \quad (6)$$

where μ_l and σ_l are the mean and variance of each batch on layer l . On training generator by inversion, batch normalization statistics contributed mostly to generating realistic images. As can be seen in Figure 4c, training without batch normalization ends with generating unrealistic images, though its loss on other losses was low.

Total variance loss. One of the common prior on natural images is that they have local smoothness, i.e., small total variance. To enforce the local smoothness of a generated image, we have used the total variance loss defined as:

$$\ell_{\text{tv}}(B) = \sum_{(i,j)} \sum_{(i',j') \in \delta(i,j)} \|G(z,y)_{(i,j)} - G(z,y)_{(i',j')}\|_2^2, \quad (7)$$

where $\delta(i, j)$ indicates a set of pixels adjacent to pixel (i, j) . The subscript indexes the generated pixel at a corresponding location.

3.2 Filtration

Our algorithm unlearns D_e by using the approximated dataset D' sampled from the trained generator G . As we enforce the diversity of outputs from G , some of the samples might not be similar to any image in the original dataset D . To further refine the generated images, we only incorporate samples whose (i) classification entropy with augmentation are lower than a pre-defined threshold t_{ent} ; and (ii) predicted labels are consistent with and without augmentation. For those samples satisfying the two criteria, we use the predicted probability as a soft-label for the generated image. Formally, the approximated dataset D' consists of

$$D' = \left\{ (G(z,y), f_w(G(z,y))) : \begin{array}{l} \forall \phi_\ell \in \phi, H(f_w(\phi_\ell(G(z,y)))) < t_{\text{ent}}, \\ \arg \max f_w(\phi_\ell(G(z,y))) = \arg \max f_w(G(z,y)) \end{array} \right\}, \quad (8)$$

where z and y are randomly sampled noise and label, respectively.

The approximated dataset D' may contain images similar to those in D_e . We need to filter out D_e -like samples from D' to retrain the classification model to unlearn D_e . We use distance-based filtering to find D_e -like samples. Specifically, we measure the distance between the generated images and the images in $D_{e,\rho}$ in its behavior and output instead of the input space, and remove the images under a certain distance threshold t_f . Formally, the set of D_e -like samples is constructed by

$$D'_e = \left\{ (x, y) : \forall (x, y) \in D', \sum_{(x_e, y_e) \in D_{e,\rho}} k(f_e(x), f_e(x_e)) < t_f \right\}, \quad (9)$$

where f_e is a feature extractor and k is a distance metric, for which an RBF kernel is employed in this work. For the feature extractor, the target classifier's output of the last convolution layer is used, followed by fully connected layers. Noting that $\sum_{(x_e, y_e) \in D_{e,\rho}} k(f_e(x), f_e(x_e))$ is a measure of similarity between $D_{e,\rho}$ and (x, y) , we set a knee point of the measure distribution over all $(x, y) \in D'$ to be an appropriate threshold t_f , c.f., Figure 4a. More specifically, we employ a knee point detection mechanism [26]. Further details are provided in Appendix C.3

Finally, we use $D'_r = D' \setminus D'_e$ as the remaining data for unlearning. Relearning only with D'_r can fail to unlearn when f_{w_o} is over-fitted to D_e , therefore, D'_e should be included. From the goal of unlearning, it is desirable to have a prediction of D_e as 0 on target classes. With this intuition, D'_e can be reformulated and included in relearning process by setting

$$D_{\text{unlearn}} = D'_r \cup \{(x, y') : \forall (x, y) \in D'_e, y' = r(y, y_e)\}, \quad (10)$$

where $r(y, y_e)$ is a soft-max function of y with the output of the label y_e as 0. Our unlearning is completed by retraining D_{unlearn} from f_{w_o} with the same training algorithm minimizing the loss in equation 1.

4 Experiment

We compare the models from a set of unlearning methods, described in what follows:

- *Original* denotes the model trained with D in advance of unlearning, i.e., no unlearning.
- *Oracle* is an ideal reference model that is fine-tuned with complete D_r initialized at the original w_o . An unlearning method can be numerically assessed by measuring the discrepancy between the behaviors of the oracle and its output model, whereas a better unlearning method has a smaller discrepancy to the oracle.
- *Ours* is from our few-shot unlearning method with the generator trained from scratch in Section 3.1
- *Ours+* is also from our method but using a pre-trained generator, which may produce more plausible samples than those from our model inversion.
- *EUBO* and *RKL* are unlearned by two different methods of variational Bayesian unlearning framework proposed in [23]. We use the suggested choice of $\lambda = 0$ for unlearning with Bayesian neural networks.
- *Fisher₁* and *Fisher₂* are from the same unlearning method proposed in [12] but with different optimizations of λ for a fair comparison. To be specific, noting that larger λ implies stronger unlearning, *Fisher₁* uses a minimal value of λ which maintains the accuracy on D_r at a certain level, i.e., a conservative unlearning. Meanwhile, *Fisher₂* uses a maximal value of λ showing a certain level of unlearning, i.e., an aggressive unlearning. Further details of the selecting *Fisher₁* and *Fisher₂* are provided in Appendix C.1.

4.1 Synthetic Moon Classification

To begin with, we verify Ours in a simple scenario of few-shot unlearning with a synthetic dataset, described in Figure 2a. In Figure 2b, we provide a fair¹ comparison of Ours and EUBO, when given complete D_e (shown in red in Figure 2a), both of them unlearn the target behavior on D_e as

¹We use the same setting of [23] including the same choice of hyperparameter $\lambda = 10^{-9}$ for their methods.

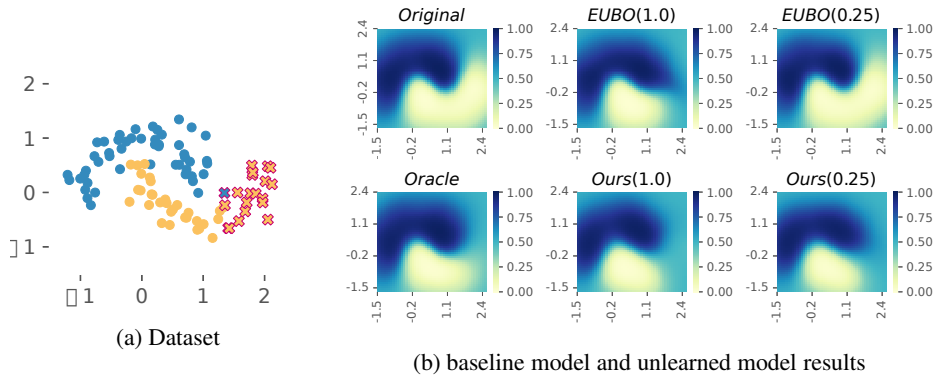


Figure 2: **Moon classification example.** Demonstration of various methods on few-shot unlearning setting. We use the same model (sparse GP model [24]) used in [23]. (a) We visualize 100 input data points defined in \mathbb{R}^2 , where each data point is colored based on its binary label. Blue and yellow are used to denote positive and negative classes respectively. The target data points are denoted as a red cross, which are originally labeled as a negative class. (b) We show the prediction over the input domain after unlearning. Only 25% of the target data points are used for unlearning.

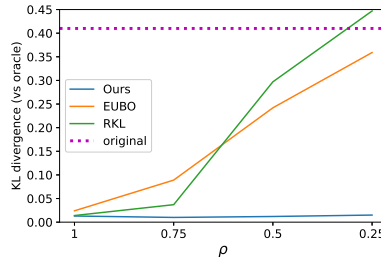


Figure 3: **KL divergence on few-shot unlearning.** Showing the KL divergence of prediction probabilities between unlearned model and oracle with various ρ . $\lambda = 10^{-9}$ is used for both EUBO and RKL which is recommended in [23].

Table 1: **KL divergence between the models when $\rho = 0.25$.** Average KL divergence between prediction probabilities of an unlearned model and two baseline models is reported. For the variational Bayesian unlearning methods, EUBO and RKL, we report the results with three different value of hyperparameter λ . For calculating KL divergence after unlearning, all data points are used.

λ	Ours	EUBO			RKL		
		10^{-5}	10^{-9}	0	10^{-5}	10^{-9}	0
vs original	0.306	0.004	0.012	0.008	0.003	0.007	0.012
vs oracle (\downarrow)	0.015	0.394	0.313	0.340	0.432	0.348	0.304

successful as Oracle does. Our method with only 5 data points ($\rho = 0.25$) yields a classifier almost identical to the oracle, whereas EUBO fails.

Along with the qualitative visualization of unlearning results, Table 1 presents a quantitative comparison in terms of KL divergence to Oracle while varying ρ . It is clear that our method gets almost zero on the KL divergence regardless of ρ . However, both EUBO and RKL have almost zero divergences only when the full dataset is given, and their gap to Oracle increases as ρ decreases, i.e., failing to few-shot unlearning.

4.2 MNIST classification

We conduct an experiment on unlearning for image classification with neural networks to show the compatibility of our method with complicated models. Here, we demonstrate the performance of unlearning methods on full-shot and few-shot (3%) settings. To perform unlearning methods, we consider two possible scenarios: 1) unlearning a whole class and 2) unlearning a subset of data.

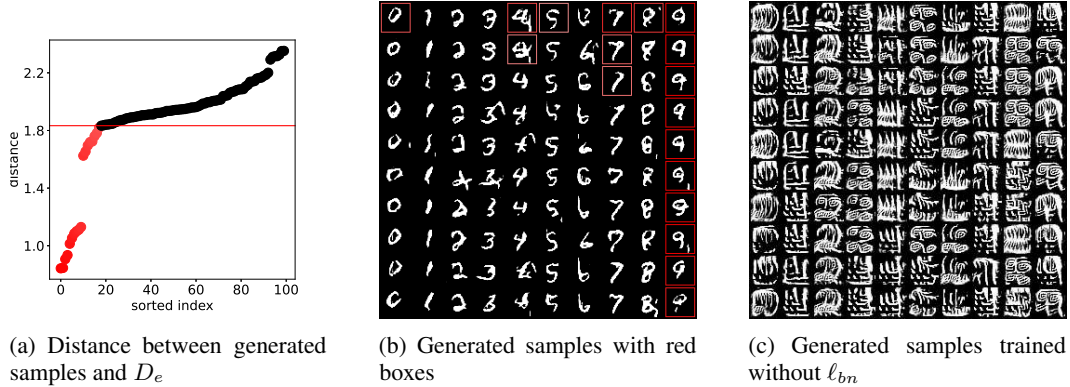


Figure 4: **Example of generated samples.** (a) We show the distances of generated samples from the target data points in D_e in ascending order, calculated with RBF kernel. The horizontal line indicates the filtration threshold found by knee point detection. Given task is to delete a class 9 from MNIST classifier. (b) Visualization of sampled images. Filtered samples are shown with the box, whose color represents the distance in (a). Box with lighter color represents bigger in distance, closer to threshold. (c) Generated samples from generator trained without ℓ_{bn} . Without ℓ_{bn} , the generator is unlikely to sample realistic images.

For the first scenario, we aim to unlearn the whole class of 9, expecting to have a low prediction probability on 9. For the second scenario, we aim to unlearn the samples with incorrect labels used for training with the original model. The second task is more involved, as it is required to maintain prediction on non-noisy data while correcting prediction over multiple classes on noisy data. Based on the observation of visual similarity among 2, 3 and 7, we modify the label of 7 to 2, 3, and 7 uniformly random for the second task. For both scenarios, we trained PreActResNet-18 [17] as a classification model. We use the DCGAN [25] and conditional GAN [22] based generator. To perform the variational Bayesian unlearning methods, we change the last layer of the classifier to the Bayesian layer used in [23] since the unlearning methods only work with Bayesian models.

We first visualize the distribution over distances from generated samples to $D_{e,p}$ in Figure 4a and the corresponding generated samples in Figure 4b. The threshold t_f for filtration is automatically detection by the knee point detection [26] from the distribution. Figure 4b shows the examples of generated and filtered samples indicated with a red box. While all data from class 9 is filtered, it can be seen that data that resemble 9 from the other classes are also filtered. Figure 4c shows generated samples when ℓ_{bn} is not used to train the generator. ℓ_{bn} is indispensable for generating plausible samples. Further ablation studies about the other losses and distance metrics are provided in Appendix E.

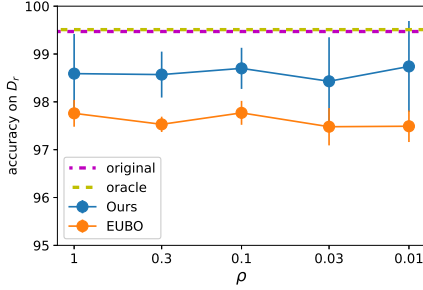
Table 2 reports the test accuracy of each model after unlearning. We note that from the difference between the scenarios the accuracy on D_e being low is better with Table 2a and high is better with Table 2b. Ours+ shows the most similar performance with the oracle in accuracy on both D_r and D_e . Ours performs slightly lower than Ours+, however, it works on general cases where a pre-trained generator is not available. We report that Fisher method fails to unlearn in neural networks. EUBO clearly erases D_e , but the accuracy on D_r drops catastrophically. RKL maintains the accuracy on D_r , but the accuracy on D_e decreases slightly. On few-shot unlearning, all results are similar to full-shot unlearning. In Table 2b, we also get a similar result to Table 2a. Our algorithm outperforms previous methods on both full-shot and few-shot unlearning.

We further check the performance of the previous model when the validation for hyperparameter is available. The results from fine-tuned EUBO and Ours on varying ρ are shown in Figure 5. Although we do not report the result here, except for EUBO, every other method failed to unlearn D_e while preserving accuracy on D_r even with the validation. We can see the accuracy on D_r of both Ours and EUBO are slightly lower than original and oracle. However, accuracy of Ours on D_e is almost the same as the oracle for all ρ , whereas, EUBO fails to unlearn when ρ is small.

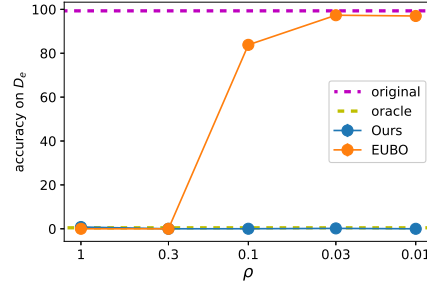
²As Fisher method failed to erase mislabeled 7 for all hyperparameters, it is impossible to report Fisher₂.

Table 2: **Test accuracy on MNIST dataset.** (a) Test accuracy of unlearned models for unlearning class of 9 in MNIST. (b) Test accuracy of unlearned models for unlearning mislabeled 7 in MNIST. Because we unlearn mislabeled data, the high accuracy on D_e is better. We repeat all experiments 5 times to report mean/std. Detailed hyperparameters used for training generator and classifier are provided in Appendix C.4.

(a) unlearning class of 9 in MNIST			(b) unlearning mislabeled 7 in MNIST		
Method	Accuracy		Method	Accuracy	
	D_r (\uparrow)	D_e (\downarrow)		D_r (\uparrow)	D_e (\uparrow)
Original	99.47	99.31	Original	98.68	37.96
Oracle	99.51	0.46	Oracle	99.54	100.00
full-shot unlearning			full-shot unlearning		
Fisher ₁	96.56 \pm 1.39	98.12 \pm 1.15	Fisher ₁	99.66 \pm 0.05	39.70 \pm 4.55
Fisher ₂	13.68 \pm 5.65	0.76 \pm 1.70	Fisher ₂ ²	-	-
EUBO	29.61 \pm 1.16	0.00 \pm 0.00	EUBO	18.81 \pm 0.80	0.00 \pm 0.00
RKL	97.62 \pm 0.37	75.53 \pm 3.32	RKL	97.29 \pm 0.46	93.30 \pm 2.68
Ours+	99.26 \pm 0.11	0.06 \pm 0.08	Ours+	99.17 \pm 0.14	97.81 \pm 1.66
Ours	99.06 \pm 0.28	0.81 \pm 1.58	Ours	99.06 \pm 0.28	96.94 \pm 2.40
few-shot (3%) unlearning			few-shot (3%) unlearning		
Fisher ₁	96.62 \pm 1.30	98.12 \pm 1.18	Fisher ₁	99.66 \pm 0.05	38.54 \pm 4.97
Fisher ₂	20.04 \pm 6.66	0.62 \pm 1.39	Fisher ₂	-	-
EUBO	35.67 \pm 1.51	0.00 \pm 0.00	EUBO	36.96 \pm 0.53	0.00 \pm 0.00
RKL	97.57 \pm 0.17	75.46 \pm 4.36	RKL	97.20 \pm 0.16	91.36 \pm 1.35
Ours+	99.43 \pm 0.07	0.08 \pm 0.07	Ours+	98.97 \pm 0.12	97.52 \pm 1.19
Ours	98.43 \pm 0.92	0.18 \pm 0.27	Ours	99.27 \pm 0.08	97.52 \pm 1.50



(a) Accuracy on D_r



(b) Accuracy on D_e

Figure 5: **Accuracy on D_r and D_e at unlearning a class of 9 with varying ρ .** EUBO reports the unlearned model with fine-tuned where $\lambda = 10^{-2410}$, which is impossible to get without validation dataset.

4.3 CIFAR-10 classification

We conduct an unlearning on CIFAR-10 dataset, which is more challenging than MNIST dataset as it contains more realistic images. We consider the scenario that aims to unlearn the whole class of ‘truck’. Overall settings for unlearning on CIFAR-10 are the same as those used in Section 4.2. The generated images shown in Figure 6a are not as clear as the images of 4.2, but we can still successfully unlearn the target data while maintaining the accuracy of the other classes, as shown in Figure 6b. We provide additional experiments on other classifier models in Appendix D.1.



(a) Generated samples in CIFAR-10 dataset.

(b) Unlearning class of ‘truck’ in CIFAR-10

Method	Accuracy	
	D_r (\uparrow)	D_e (\downarrow)
Original	93.24	96.10
Oracle	93.47	2.40
full-shot unlearning		
Fisher ₁	91.80 ± 0.42	95.80 ± 0.57
Fisher ₂	13.60 ± 2.52	0.00 ± 0.00
EUBO	12.26 ± 0.65	0.00 ± 0.00
RKL	87.33 ± 0.15	70.04 ± 2.85
Ours+	89.61 ± 0.49	0.00 ± 0.00
Ours	88.73 ± 0.54	0.32 ± 0.28
few-shot (3%) unlearning		
Fisher ₁	91.73 ± 0.41	95.78 ± 0.63
Fisher ₂	13.60 ± 4.51	0.00 ± 0.00
EUBO	24.46 ± 0.48	0.01 ± 0.00
RKL	87.23 ± 0.07	68.50 ± 2.93
Ours+	89.79 ± 0.29	0.00 ± 0.00
Ours	88.52 ± 0.32	0.52 ± 0.17

Figure 6: **Overall unlearning results on CIFAR-10.** (a) Visualization of sampled images. Each column contains the samples with the same label. (b) Test accuracy of unlearned models for unlearning class of ‘truck’ on CIFAR-10.

5 Conclusion

We have proposed a few-shot unlearning method to erase a target behavior from a trained model given a few target examples. Our method consists of two parts: inverting the model to retrieve training data and relearning with the retrieved data after excluding data similar to the target examples. We demonstrate training a generator without access to any data by model inversion. The proposed model inversion technique is not limited to unlearning but can be applied for other uses, e.g., data-free transfer learning [30]. There might be a concern about privacy leakage by our model inversion technique. However, the experimental results show that it is sufficient to have roughly generated images for successful unlearning. Although our method uses only a subset of target data, it outperforms the state-of-the-art methods with a full indication of target data. Our method, however, is limited in probabilistic classifiers to utilize the entropy based filtering. Nevertheless, we believe that our method can be extended for other classifiers or regressors by devising a surrogate measure of data likelihood such as the sensitivity of output to small perturbation of input.

References

- [1] Thomas Baumhauer, Pascal Schöttle, and Matthias Zeppelzauer. Machine unlearning: Linear filtration for logit-based classifiers. *arXiv preprint arXiv:2002.02730*, 2020.
- [2] Lucas Bourtole, Varun Chandrasekaran, Christopher A Choquette-Choo, Hengrui Jia, Adelin Travers, Baiwu Zhang, David Lie, and Nicolas Papernot. Machine unlearning. *arXiv preprint arXiv:1912.03817*, 2019.
- [3] Yinzhi Cao and Junfeng Yang. Towards making systems forget with machine unlearning. In *2015 IEEE Symposium on Security and Privacy*, pages 463–480. IEEE, 2015.
- [4] Hanting Chen, Yunhe Wang, Chang Xu, Zhaohui Yang, Chuanjian Liu, Boxin Shi, Chunjing Xu, Chao Xu, and Qi Tian. Data-free learning of student networks. In *Proceedings of the IEEE/CVF International Conference on Computer Vision*, pages 3514–3522, 2019.
- [5] Yoojin Choi, Jihwan Choi, Mostafa El-Khamy, and Jungwon Lee. Data-free network quantization with adversarial knowledge distillation. In *Proceedings of the IEEE/CVF Conference on Computer Vision and Pattern Recognition Workshops*, pages 710–711, 2020.
- [6] Vikram S Chundawat, Ayush K Tarun, Murari Mandal, and Mohan Kankanhalli. Zero-shot machine unlearning. *arXiv preprint arXiv:2201.05629*, 2022.
- [7] Min Du, Zhi Chen, Chang Liu, Rajvardhan Oak, and Dawn Song. Lifelong anomaly detection through unlearning. In *Proceedings of the 2019 ACM SIGSAC Conference on Computer and Communications Security*, pages 1283–1297, 2019.
- [8] Matt Fredrikson, Somesh Jha, and Thomas Ristenpart. Model inversion attacks that exploit confidence information and basic countermeasures. In *Proceedings of the 22nd ACM SIGSAC conference on computer and communications security*, pages 1322–1333, 2015.
- [9] Shaopeng Fu, Fengxiang He, Yue Xu, and Dacheng Tao. Bayesian inference forgetting. *arXiv preprint arXiv:2101.06417*, 2021.
- [10] Antonio Ginart, Melody Guan, Gregory Valiant, and James Y Zou. Making ai forget you: Data deletion in machine learning. *Advances in Neural Information Processing Systems*, 32, 2019.
- [11] Aditya Golatkar, Alessandro Achille, Avinash Ravichandran, Marzia Polito, and Stefano Soatto. Mixed-privacy forgetting in deep networks. In *Proceedings of the IEEE/CVF Conference on Computer Vision and Pattern Recognition*, pages 792–801, 2021.
- [12] Aditya Golatkar, Alessandro Achille, and Stefano Soatto. Eternal sunshine of the spotless net: Selective forgetting in deep networks. In *Proceedings of the IEEE/CVF Conference on Computer Vision and Pattern Recognition*, pages 9304–9312, 2020.
- [13] Ian Goodfellow, Jean Pouget-Abadie, Mehdi Mirza, Bing Xu, David Warde-Farley, Sherjil Ozair, Aaron Courville, and Yoshua Bengio. Generative adversarial nets. *Advances in neural information processing systems*, 27, 2014.
- [14] Laura Graves, Vineel Nagisetty, and Vijay Ganesh. Amnesiac machine learning. *arXiv preprint arXiv:2010.10981*, 2020.
- [15] Chuan Guo, Tom Goldstein, Awni Hannun, and Laurens Van Der Maaten. Certified data removal from machine learning models. *arXiv preprint arXiv:1911.03030*, 2019.
- [16] Varun Gupta, Christopher Jung, Seth Neel, Aaron Roth, Saeed Sharifi-Malvajerdi, and Chris Waites. Adaptive machine unlearning. *arXiv preprint arXiv:2106.04378*, 2021.
- [17] Kaiming He, Xiangyu Zhang, Shaoqing Ren, and Jian Sun. Deep residual learning for image recognition. In *Proceedings of the IEEE conference on computer vision and pattern recognition*, pages 770–778, 2016.
- [18] Jinwoo Jeon, Kangwook Lee, Sewoong Oh, Jungseul Ok, et al. Gradient inversion with generative image prior. *Advances in Neural Information Processing Systems*, 34:29898–29908, 2021.
- [19] Yann LeCun, Léon Bottou, Yoshua Bengio, and Patrick Haffner. Gradient-based learning applied to document recognition. *Proceedings of the IEEE*, 86(11):2278–2324, 1998.
- [20] Liangchen Luo, Mark Sandler, Zi Lin, Andrey Zhmoginov, and Andrew Howard. Large-scale generative data-free distillation. *arXiv preprint arXiv:2012.05578*, 2020.

- [21] Alessandro Mantelero. Right to be forgotten and public registers-a request to the european court of justice for a preliminary ruling. *Eur. Data Prot. L. Rev.*, 2:231, 2016.
- [22] Mehdi Mirza and Simon Osindero. Conditional generative adversarial nets. *arXiv preprint arXiv:1411.1784*, 2014.
- [23] Quoc Phong Nguyen, Bryan Kian Hsiang Low, and Patrick Jaillet. Variational bayesian unlearning. *Advances in Neural Information Processing Systems*, 33, 2020.
- [24] Joaquin Quinonero-Candela and Carl Edward Rasmussen. A unifying view of sparse approximate gaussian process regression. *The Journal of Machine Learning Research*, 6:1939–1959, 2005.
- [25] Alec Radford, Luke Metz, and Soumith Chintala. Unsupervised representation learning with deep convolutional generative adversarial networks. *arXiv preprint arXiv:1511.06434*, 2015.
- [26] Ville Satopaa, Jeannie Albrecht, David Irwin, and Barath Raghavan. Finding a" kneedle" in a haystack: Detecting knee points in system behavior. In *2011 31st international conference on distributed computing systems workshops*, pages 166–171. IEEE, 2011.
- [27] Ayush K Tarun, Vikram S Chundawat, Murari Mandal, and Mohan Kankanhalli. Fast yet effective machine unlearning. *arXiv preprint arXiv:2111.08947*, 2021.
- [28] Ziqi Yang, Ee-Chien Chang, and Zhenkai Liang. Adversarial neural network inversion via auxiliary knowledge alignment. *arXiv preprint arXiv:1902.08552*, 2019.
- [29] Hongxu Yin, Pavlo Molchanov, Jose M Alvarez, Zhizhong Li, Arun Mallya, Derek Hoiem, Niraj K Jha, and Jan Kautz. Dreaming to distill: Data-free knowledge transfer via deepinversion. In *Proceedings of the IEEE/CVF Conference on Computer Vision and Pattern Recognition*, pages 8715–8724, 2020.
- [30] Jaemin Yoo, Minyong Cho, Taebum Kim, and U Kang. Knowledge extraction with no observable data. *Advances in Neural Information Processing Systems*, 32, 2019.
- [31] Xinyi YU, Ling Yan, and Linlin Ou. Conditional generative data-free knowledge distillation based on attention transfer. *arXiv preprint arXiv:2112.15358*, 2021.
- [32] Haoran Zhao, Xin Sun, Junyu Dong, Milos Manic, Huiyu Zhou, and Hui Yu. Dual discriminator adversarial distillation for data-free model compression. *International Journal of Machine Learning and Cybernetics*, 13(5):1213–1230, 2022.

A Proposed methods

In this section, for clarity, we provide pseudo codes of the propose methods: Algorithm 1 for training generative model approximating D ; and Algorithm 2 for obtaining dataset D' . Algorithm 3 filters obtained dataset D' to unlearning dataset D_{unlearn} , and Algorithm 4 unlearns classifier by D_{unlearn} .

Algorithm 1 Training generator

Input: classifier: C ,
generator: G ,
augmentation: $\Phi = \{\phi_1, \phi_2, \dots, \phi_k\}$
Output: Trained generator: G

initialize G
repeat
 $z \leftarrow N(0, I)$
 $y \leftarrow \text{random int}[0, \text{number of classes}]$
 $x \leftarrow G(z, y)$.
 Augment x by $\phi_1, \phi_2, \dots, \phi_k$
 Train G with losses defined in subsection 3.1.
until G converges.
return G

Algorithm 2 Generating data

Input: classifier: C ,
generator: G ,
augmentation: $\Phi = \{\phi_1, \phi_2, \dots, \phi_k\}$
Output: Approximated dataset: D'

$D' \leftarrow []$
repeat
 for y_i in classes **do**
 $Z \leftarrow N(0, I)$
 $Y \leftarrow y_i$
 $X \leftarrow G(Z, Y)$.
 for $x \in X$ **do**
 if $H(x) > t_{\text{ent}}$ **then**
 delete x
 end if
 for $\phi \in \Phi$ **do**
 if $\arg \max_y(C(x)) \neq \arg \max_y(C(\phi(x)))$ **then**
 delete x
 end if
 end for
 end for
 $D'.\text{append}(X, C(X))$
 end for
until Proper number of data is generated
return D'

Algorithm 3 Filtering dataset

Input: data to erase: D_e
feature extractor: f_e ,
distance metric: k
knee detection algorithm: $knee$
target classes: Y_{target}

Output: Filtered dataset: $D_{unlearn}$

Thresholding

distances $\leftarrow []$
for $d' \in D'$ **do**
 distance $\leftarrow k(f_e(d'), f_e(D_e))$
 distances.append(distance)
end for
threshold $\leftarrow knee(distances)$

Filtering

$D_{unlearn} \leftarrow []$
for $d' \in D'$ **do**
 data, label $\leftarrow d'$
 if threshold $> k(f_e(d'), f_e(D_e))$ **then**
 for $y_{target} \in Y_{target}$ **do**
 label[y_{target}] = 0
 end for
 end if
 $d_{unlearn} \leftarrow \text{data, label}$
 $D_{unlearn}.append(d_{unlearn})$
end for

return $D_{unlearn}$

Algorithm 4 Unlearning classifier

Input: classifier: C ,
dataset: $D_{unlearn}$
augmentation: $\Phi = \{\phi_1, \phi_2, \dots, \phi_k\}$

Output: Unlearned classifier: C_{D_r}

repeat
 for batch in $D_{unlearn}$ **do**
 inputs, labels \leftarrow batch
 outputs $\leftarrow C(\text{inputs})$
 loss $\leftarrow CE(\text{outputs}, \text{labels})$
 update C
 end for
until C converges.

return C

B Time Complexity of Unlearning Methods

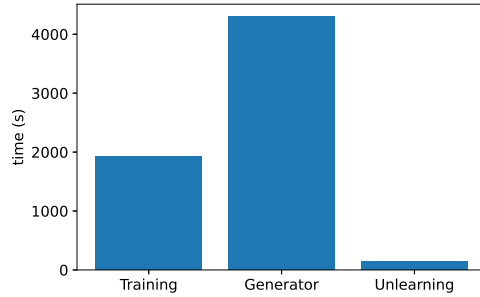


Figure 7: **Required time for training and unlearning by our method.** Training is the time to train the Original model. Generator is the time to train a generator for our method. Unlearning is the time to unlearn D_e with trained generator. Time is measured for the few-show unlearning (3%) task, which unlearning a class of 9 in MNIST.

We plot the required time for training a proposed generator and unlearning the original classifier in Figure 7. Although it takes a relatively long time to train the generator, it may be not a long time as collecting a new dataset in a real-world situation will takes a longer time. As Appendix D.2 shows, it may be faster in situations such as sequential unlearning or continual learning because the generator can be recycled. All our experiments are performed on GPU servers equipped with NVIDIA RTX A6000.

C Hyperparameter Selection

C.1 λ selection on Fisher

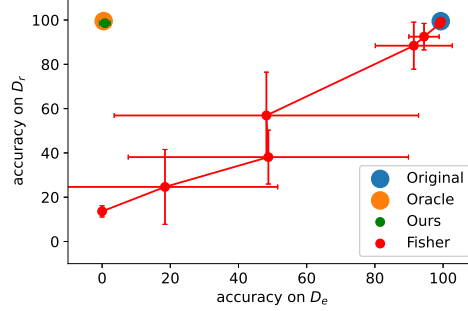


Figure 8: **Accuracy on D_r and D_e at unlearning a class of 9 in MNIST with varying λ .** We use the $\lambda = 1.0 \times 10^{-8}, 5.0 \times 10^{-8}, 1.0 \times 10^{-7}, 1.5 \times 10^{-7}, 2.0 \times 10^{-7}, 2.5 \times 10^{-7}, 3.0 \times 10^{-7}, 3.5 \times 10^{-7}$, which plotted the upper right side to the lower left side. We repeat this experiment 5 times to report mean/std.

In Figure 8, Original is located on the upper right side, which means both the accuracy on D_r and D_e is high. Oracle shows the accuracy on D_e smaller than Original and is located on the left side of Original. As Ours gets outstanding unlearning performance, erasing D_e clearly while retaining D_r , Ours is located close to Oracle. Fisher starts at Original, however, as λ grows, moves to the lower left side, meaning that D_e is erased while D_r is also erased. Moreover, any value of λ could not make Fisher reach Oracle. It is hard to choose the best one for reporting results, thus, we use Fisher₁ and Fisher₂ in Section 4.

C.2 Entropy Threshold t_{ent} Selection

Table 3: **Test accuracy on varying entropy threshold t_{ent} .** Test accuracy of unlearned models for unlearning class of 9 in MNIST on varying t_{ent} . We use $t_{\text{ent}} = 0.282, 0.500, 0.867$, which are entropy of $[0.82, 0.02, \dots, 0.02]$, and $[0.91, 0.01, \dots, 0.01]$, $[0.955, 0.005, \dots, 0.005]$. We repeat all experiments 5 times to report mean/std.

Method	Accuracy	
	D_r (\uparrow)	D_e (\downarrow)
Original	99.47	99.31
Oracle	99.51	0.46
full-shot unlearning		
$t_{\text{ent}} = 0.282$	98.63 ± 0.55	0.00 ± 0.00
$t_{\text{ent}} = 0.500^3$	99.26 ± 0.11	0.06 ± 0.08
$t_{\text{ent}} = 0.867$	98.37 ± 0.25	0.00 ± 0.00
few-shot (3%) unlearning		
$t_{\text{ent}} = 0.282$	98.61 ± 0.54	0.00 ± 0.00
$t_{\text{ent}} = 0.500$	99.43 ± 0.07	0.08 ± 0.07
$t_{\text{ent}} = 0.867$	98.58 ± 0.33	0.00 ± 0.00

t_{ent} is the threshold in our method, for finding more realistic (D -like) samples in the generated samples. In Table 3, all of the unlearned model accuracy on D_r is higher than 98% and accuracy on D_e is lower than it of Oracle. When t_{ent} is big or small, the accuracy on D_r dropped slightly. However, since z is not optimized but randomly generated, there is an issue that it takes a long time to generate when t_{ent} is very small. Therefore, fine-tuning t_{ent} improves performance, but it is not such a sensitive one.

³all of other experiment used it.

C.3 Generating Data and Determining t_f

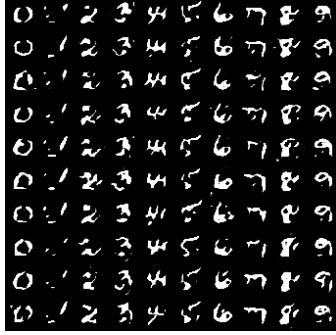
To generate D' from the generator, we use randomly sampled noise z . Optimizing the noise z is also a factor to consider, but randomly sampled noise is more efficient for both time and variant data. Furthermore, the result in Appendix C.2 shows that the data quality (entropy of the predicted output on the original model) is not an important factor in our method. Our method uses a nontrivial threshold t_f to filter whether the generated sample x is D_e -like or not on a distance metric k . An ablation study about k is provided in Appendix E.2, while we use the RBF kernel as k for every experiment. x is filtered by the sum of distances with the given D_e with threshold t_f . Determining the value of t_f is important, as it may occur remembering D_e or catastrophic forgetting on D_r . Based on the belief that the D_e -like samples are nearby in feature space while separated from the other samples, we use the knee point detection algorithm to determine t_f . Figure 4a shows the sorted distance of the generated samples and t_f from the knee point detection algorithm. Also, we can choose the proper t_f by our decision from observing the generated samples.

C.4 Hyperparameter Selection for training classifier, generator, and unlearning

To train a classifier in experiments, an SGD optimizer with a learning rate of 0.01, a momentum of 0.9, and a weight decay rate of 0.0002 are used. To train a generator, an ADAM optimizer with a learning rate of 0.002, betas of (0.5, 0.999), and weight decay rate of 0.0002 is used. For balancing between losses defined in subsection 3.1, some multiplier is used; 10.0 for Batch normalization loss, 1.0 for Entropy loss, 0.03 for Augmentation loss, 1.0 for Diversity loss, and 3.0 for total variation loss. While different hyperparameter also works, we report each value is good enough. For unlearning, an SGD optimizer with a learning rate of 0.003, a momentum of 0.9, and a weight decay rate of 0.00002 are used.

D Additional Experiments

D.1 Unlearning on Other Original Model Architectures



(a) LeNet5



(b) ResNet-50

Figure 9: **Generated samples from the generator trained with different classifier models.** Generated samples from generator trained with (a) LeNet5[19] and (b) ResNet-50[17].

Table 4: **Test accuracy on varying models.** Test accuracy of unlearned models for unlearning class of 9 of MNIST on (a) LeNet5 and (c) ResNet-50. Test accuracy of unlearned models for unlearning 7 of MNIST on (b) LeNet5 and (d) ResNet-50. We repeat all experiments 5 times to report mean/std.

(a) unlearning 9 on LeNet5			(b) unlearning 7 on LeNet5		
Method	Accuracy		Method	Accuracy	
	D_r (\uparrow)	D_e (\downarrow)		D_r (\uparrow)	D_e (\uparrow)
Original	99.31	99.20	Original	99.19	72.26
Oracle	99.34	0.00	Oracle	99.36	95.62
full-shot unlearning			full-shot unlearning		
Ours+	98.80 ± 0.04	0.44 ± 0.39	Ours+	82.16 ± 1.57	98.39 ± 0.29
Ours	98.46 ± 0.39	0.12 ± 0.07	Ours	89.26 ± 3.70	98.69 ± 0.29
few-shot (3%) unlearning			few-shot (3%) unlearning		
Ours+	98.74 ± 0.15	0.32 ± 0.25	Ours+	98.62 ± 0.07	93.28 ± 3.24
Ours	98.41 ± 0.32	0.60 ± 0.22	Ours	98.44 ± 0.24	95.33 ± 3.12
(c) unlearning 9 on ResNet-50			(d) unlearning 7 on ResNet-50		
Method	Accuracy		Method	Accuracy	
	D_r (\uparrow)	D_e (\downarrow)		D_r (\uparrow)	D_e (\uparrow)
Original	99.24	99.41	Original	99.19	17.52
Oracle	99.32	0.00	Oracle	99.72	100.00
full-shot unlearning			full-shot unlearning		
Ours+	98.99 ± 0.12	0.00 ± 0.00	Ours+	98.35 ± 0.46	98.54 ± 1.13
Ours	98.77 ± 0.40	0.02 ± 0.04	Ours	98.27 ± 0.43	98.54 ± 0.46
few-shot (3%) unlearning			few-shot (3%) unlearning		
Ours+	99.03 ± 1.13	0.00 ± 0.00	Ours+	98.98 ± 0.19	98.98 ± 0.36
Ours	98.89 ± 0.32	0.32 ± 0.32	Ours	98.64 ± 0.53	96.50 ± 1.87

We demonstrate our method on the small model (LeNet5) and the large model (ResNet-50) in Table 4. Original LeNet5 does not have a batch normalization layer, thus we add it before every convolution layer. The generated samples from the generator trained on LeNet5 and ResNet-50 are in Figure 9. Unlearning results on both mod-

els show lower performance compared to ResNet-18 in Table 2. Especially, full-shot unlearning performance in Table 4b is much lower than others, it may be the dimension of behavior in LeNet5 is not sufficient to filter 7. Although ResNet-50 is a larger model than ResNet-18, it can be seen that the accuracy of D_r is slightly lower, due to the lower accuracy of the Original.

D.2 Transferability of Generator

Table 5: **Test accuracy on other classifiers.** Test accuracy of unlearned models for few-shot (3%) unlearning in MNIST on other classifier models. We use 4 Generator and Classifier models, ResNet-18₁ and ResNet-18₂ are using same architecture ResNet-18 on different random seed. LeNet5 and ResNet-50 are used to observe the effect of the generator trained from the different classifier architectures. We repeat all experiments 5 times to report mean/std.

(a) unlearning class of 9 in MNIST.					
Classifier (\rightarrow)		ResNet-18 ₁	ResNet-18 ₂	LeNet5	ResNet-50
Generator (\downarrow)		Accuracy			
Original	D_e (\downarrow)	99.31	99.50	99.20	99.41
	D_r (\uparrow)	99.47	98.78	99.31	99.24
Oracle	D_e (\downarrow)	0.46	0.50	0.00	0.00
	D_r (\uparrow)	99.51	99.67	99.34	99.32
few-shot (3%) unlearning					
ResNet-18 ₁	D_e (\downarrow)	0.18 ± 0.27	0.06 ± 0.12	0.30 ± 0.06	0.16 ± 0.15
	D_r (\uparrow)	98.43 ± 0.92	99.38 ± 0.09	98.56 ± 0.61	99.32 ± 0.17
ResNet-18 ₂	D_e (\downarrow)	0.00 ± 0.00	0.00 ± 0.00	2.81 ± 5.29	0.00 ± 0.00
	D_r (\uparrow)	98.53 ± 0.66	99.15 ± 0.15	98.14 ± 0.28	98.97 ± 0.26
LeNet5	D_e (\downarrow)	0.06 ± 0.08	0.24 ± 0.26	0.60 ± 0.22	0.16 ± 0.12
	D_r (\uparrow)	98.19 ± 0.76	99.36 ± 0.16	98.41 ± 0.32	99.28 ± 0.14
ResNet-50	D_e (\downarrow)	31.42 ± 21.20	40.63 ± 22.33	12.37 ± 9.50	0.32 ± 0.32
	D_r (\uparrow)	99.20 ± 0.22	99.26 ± 0.28	98.22 ± 0.44	98.89 ± 0.32
(b) unlearning 7 in MNIST					
Classifier (\rightarrow)		ResNet-18 ₁	ResNet-18 ₂	LeNet5	ResNet-50
Generator (\downarrow)		Accuracy			
Original	D_e (\uparrow)	37.96	55.47	72.26	17.52
	D_r (\uparrow)	98.68	99.45	99.19	99.19
Oracle	D_e (\uparrow)	100.00	99.27	95.62	100.00
	D_r (\uparrow)	99.54	99.67	99.36	99.72
few-shot (3%) unlearning					
ResNet-18 ₁	D_e (\uparrow)	97.52 ± 1.50	99.85 ± 0.33	99.42 ± 0.95	99.85 ± 0.33
	D_r (\uparrow)	99.27 ± 0.08	99.14 ± 0.17	83.04 ± 8.33	97.79 ± 1.25
ResNet-18 ₂	D_e (\uparrow)	94.89 ± 5.06	98.83 ± 1.22	82.63 ± 11.59	97.23 ± 0.95
	D_r (\uparrow)	99.30 ± 0.13	98.56 ± 0.51	98.49 ± 0.48	99.21 ± 0.11
LeNet5	D_e (\uparrow)	94.60 ± 5.50	99.27 ± 0.33	95.33 ± 3.12	100.00 ± 0.00
	D_r (\uparrow)	99.44 ± 0.06	99.21 ± 0.18	98.44 ± 0.24	99.10 ± 0.48
ResNet-50	D_e (\uparrow)	96.06 ± 3.37	100.00 ± 0.00	99.27 ± 0.52	96.50 ± 1.87
	D_r (\uparrow)	99.34 ± 0.12	99.42 ± 0.14	97.45 ± 1.50	98.64 ± 0.53

In this experiment, we test the transferability of the generator, by unlearning the target classifier with the generator trained from another classifier. Except for the case of the Generator trained from the classifier modeled ResNet-50 in Table 5a, our method can get a similar performance to Oracle model. However, it failed when using the complex model, ResNet-50, probably because the ResNet-50 is too large for regularization, so the generator generated only a few '9's, i.e. due to the lack of diversity on D_e .

E Ablation Studies

E.1 Ablation Study for Generator Losses

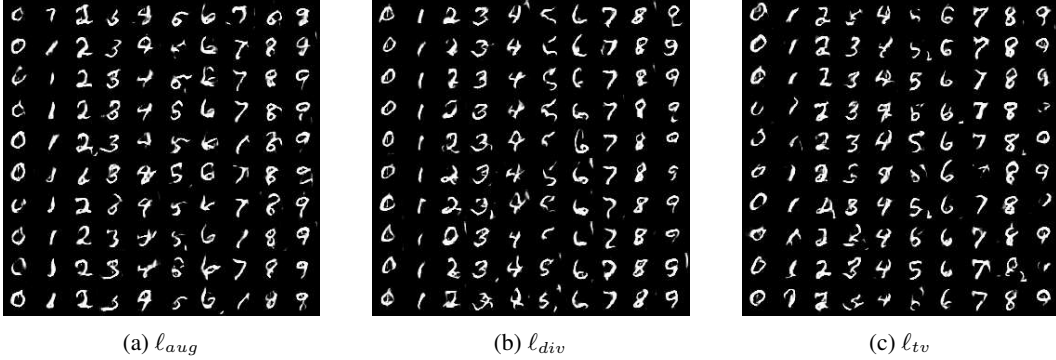


Figure 10: **Generated samples from the generator trained without each generator losses.** Generated samples from generator trained without (a) ℓ_{aug} , (b) ℓ_{div} , and (c) ℓ_{tv} .

Table 6: **Test accuracy on the sample from the each generator trained without ℓ .** Test accuracy of unlearned models for unlearning class of 9 in MNIST with each generator. G_{full} is the generator trained with all proposed losses, $G_{-\ell_i}$ is the generator trained without ℓ_i . We repeat all experiments 5 times to report mean/std.

Method	Accuracy	
	D_r (\uparrow)	D_e (\downarrow)
Original	99.47	99.31
Oracle	99.51	0.46
full-shot unlearning		
G_{full}	99.26 ± 0.11	0.06 ± 0.08
$G_{-\ell_{bn}}$	94.34 ± 1.01	93.54 ± 2.64
$G_{-\ell_{aug}}$	98.93 ± 0.36	0.00 ± 0.00
$G_{-\ell_{div}}$	98.89 ± 0.14	0.00 ± 0.00
$G_{-\ell_{tv}}$	99.07 ± 0.09	0.00 ± 0.00
few-shot (3%) unlearning		
G_{full}	99.43 ± 0.07	0.08 ± 0.07
$G_{-\ell_{bn}}$	94.72 ± 0.61	89.40 ± 2.64
$G_{-\ell_{aug}}$	99.13 ± 0.10	0.00 ± 0.00
$G_{-\ell_{div}}$	98.77 ± 0.38	0.00 ± 0.00
$G_{-\ell_{tv}}$	98.74 ± 0.27	0.00 ± 0.00

We use 5 losses, ℓ_{ent} , ℓ_{aug} , ℓ_{div} , ℓ_{bn} , and ℓ_{tv} , to train the generator. As ℓ_{ent} is essential to train the conditional generator, we report an ablation study for the other generator losses. The ablation study of ℓ_{bn} is in Figure 4c. The generated samples from the ablation study about the other losses are in Figure 10. It seems similar in human-view, but the unlearning performance gap is reported in Table 6. Except for $G_{-\ell_{bn}}$, the others achieve similar performance with G_{full} on both full-shot and few-shot unlearning. As the sample generated by $G_{-\ell_{bn}}$ is strange, it can be seen that the unlearning did not proceed well.

E.2 Ablation Study for Distance Metrics

We use the RBF kernel to filter D_e -like samples in D' in all experiments. As RBF kernel is the sum of the Gaussian probability from each data point in a given D_e , it has the advantages of robustness on the shape of behavior distribution of D_e -like samples. In Table 7, the RBF kernel is compared with L2-norm and cosine

⁴all of other experiment used it.

Table 7: **Test accuracy on Distance Metric k .** Test accuracy of unlearned models for unlearning class of 9 in MNIST on varying distance metric k . We use RBF kernel, cosine similarity, and l2-norm as k . We repeat all experiments 5 times to report mean/std.

Method	Accuracy	
	D_r (\uparrow)	D_e (\downarrow)
Original	99.47	99.31
Oracle	99.51	0.46
full-shot unlearning		
RBF ⁴	99.26 ± 0.11	0.06 ± 0.08
cosine	98.81 ± 0.15	0.00 ± 0.00
l2-norm	98.59 ± 0.51	0.00 ± 0.00
few-shot (3%) unlearning		
RBF	99.43 ± 0.07	0.08 ± 0.07
cosine	98.85 ± 0.27	0.00 ± 0.00
l2-norm	98.13 ± 0.27	0.00 ± 0.00

similarity, which are mainly used for measuring the distance between behaviors. RBF maintains the highest accuracy on D_r , while the others also maintain high accuracy after erasing D_e .